in the assay. The method 1 shown in Figs. 1 and 2 is equivalent to the real-time nested PCR developed by Brussel et al. and the method 2 is the new real time nested PCR we have developed. Figs. 2a and b clearly demonstrated that specificity of our novel assay (method 2) was much higher than the previously reported method using a tag sequence. The probe-2 used in method 2 could inhibit the annealing of the residual tagged primer, which resulted in higher specificity than method 1.

By this novel assay, detailed kinetics of viral DNA synthesis was analyzed in Jurkat cells. Our assay detected integrated HIV-1 DNA within 3 h of infection, which emphasizes the sensitivity of this assay.

Then, we analyzed the kinetics of HIV-1 integration in U937 cells, activated PBMC's and resting PBMC's in addition to Jurkat cells. The kinetics of viral DNA integration depended on the cell type. HIV-1 DNA integration was completed 12 h after infection in Jurkat cells and U937 cells, 24 h in activated PBMCs and 48 h in resting PBMC's. Efficiency of viral integration was correlated with activity of reverse transcription. Jurkat cells exhibited the most rapid kinetics of reverse transcription and integration, and we may find the new factor(s) associated with reverse transcription and integration by investigating the molecules up-regulated or down-regulated in Jurkat cells.

The specific, sensitive and quantitative assay we have developed should prove useful in the kinetic studies of the integrated HIV-1 DNA especiallly during the early phase of infection. It should also prove applicable to clinical studies of viral integration and assessments of the effectiveness of future integrase inhibitors. Furthermore, it may be a valuable tool to test the integration efficiency of retroviral vectors designed for gene therapies.

Acknowledgements We thank Dr. Naoki Yamamoto for his support and helpful discussions. This work was supported by grants from the Ministry of Education, Science and Culture and the Ministry of Health, Labor and Welfare of Japan.

References

1. G. Englund, T.S. Theodore, E.O. Freed, A. Engleman, M.A. Martin, J. Virol. 69, 3216–3219 (1995)
2. B.J. Brussel, C.L. Schneider, H.L. Robbins, P.L. Callahan, K. Terhorst, J. Roth, W.A. Schleif, E.A. Emini, J. Virol. 66, 7311–7319 (1992)
3. H. Sato, M. Kawamura, J. Sakuragi, S. Sakuragi, R. Shibata, A. Ishimoto, N. Ono, S. Ueda, A. Adachi, J. Virol. 67, 1169–1174 (1993)
4. M. Stevenson, T.J. Stanwick, M.P. Dempsey, C.A. Lamonica, EMBO J. 9, 1551–1560 (1990)
5. M.I. Bukrinsky, N. Sharova, M.P. Dempsey, T.L. Stanwick, A.G. Bukrinskaya, S. Haggerty, M. Stevenson, Proc. Natl. Acad. Sci. USA 89, 6580–6584 (1992)
6. M.I. Bukrinsky, N. Sharova, T.L. McDonald, T. Pushkarskaya, W.G. Tarpley, M. Stevenson, Proc. Natl. Acad. Sci. USA 90, 6125–6129 (1993)
7. C.M. Farnet, F.D. Bushman, Cell 88, 483–92 (1997)
8. J.L. Yoder, M.S. Hansen, J. Olvera, M.D. Miller, F.D. Bushman, J. Virol. 74, 10965–10974 (2000)
9. M.D. Miller, C.M. Farnet, F.D. Bushman, J. Virol. 71, 5382–5390 (1997)
10. P. Barbosa, P. Charneau, N. Dumey, F. Clavel, AIDS Res. Hum. Retroviruses 10, S3–S9 (1994)
11. S.Y. Kim, R. Byrn, J. Groopman, D. Baltimore, J. Virol. 63, 3708–3713 (1989)
12. J.W. Chun, J. Stuyver, S.B. Mizell, L.A. Ehler, J.A. Mican, M. Baseler, A.L. Lloyd, M.A. Nowak, A.S. Fauci, Proc. Natl. Acad. Sci. USA 94, 13193–13197 (1997)
13. S. Sonza, A. Maerz, N. Deacon, J. Meanger, J. Mills, S. Crowe, J. Virol. 70, 8863–8869 (1996)
14. R.J. Batten, W.F. Baron, D.B. Stout, E.H. Davidson, Proc. Natl. Acad. Sci. USA 85, 4770–4774 (1988)
15. R. Kumar, N. Vandegraaff, L. Mundy, C.J. Burrell, P. Li, J. Virol. Methods 105, 233–246 (2002)
16. N. Vandegraaff, R. Kumar, C.J. Burrell, P. Li, J. Virol. 75, 11253–11260 (2001)
17. U. O'Doherty, W.J. Swiggard, D. Jeyakumar, D. McGain, M.H. Malim, J. Virol. 76, 10942–10950 (2002)
18. A. Brussel, P. Sonigo, J. Virol. 77, 10119–10124 (2003)
19. S.L. Butler, M.S. Hansen, F.D. Bushman, Natl. Med. 7, 631–634 (2001)
20. S.L. Butler, E.P. Johnson, F.D. Bushman, J. Virol. 76, 3739–3747 (2002)

Nucleosides, Nucleotides, and Nucleic Acids, 26:815–820, 2007

ISSN: 1525-7770 print / 1532-2335 online
DOI: 10.1080/15257770701503787

Taylor & Francis
Taylor & Francis Group

SUPPRESSION OF HEPATITIS C VIRUS CORE PROTEIN BY SHORT HAIRPIN RNA EXPRESSION VECTORS IN THE CORE PROTEIN EXPRESSION HUH-7 CELLS

Hitoshi Suzuki, Hiroyasu Kaneko, and Nobushige Tamai □ *Department of Life and Environmental Sciences, Chiba Institute of Technology, Chiba, Japan*

Kunitada Shimotohno □ *Department of Viral Oncology, Institute for Virus Research, Kyoto University, Kyoto, Japan*

Naoko Miyano-Kurosaki and Hiroshi Takaku □ *Department of Life and Environmental Sciences, Chiba Institute of Technology, Chiba, Japan, and High Technology Research Center, Chiba Institute of Technology, Chiba, Japan*

□ *Short hairpin RNAs (shRNAs) efficiently inhibit gene expression by RNA interference. Here, we report the efficient inhibition by DNA-based vector-derived shRNAs of core protein expression in Huh-7 cells. The shRNAs were designed to target the core region of the hepatitis C virus (HCV) genome. The core region is the most conserved region in the HCV genome, making it an ideal target for shRNAs. We identified an effective site on the core region for suppression of the HCV core protein. The HCV core protein in core protein-expressing Huh-7 cells was downregulated by core protein-shRNA expression vectors (core-shRNA-452, 479, and 503). Our results support the feasibility of using shRNA-based gene therapy to inhibit HCV core protein production.*

Keywords RNAi; Short hairpin RNAs (shRNAs); hepatitis C virus (HCV) core protein; Huh-7 cells; GFP; DsRed

INTRODUCTION

Hepatitis C virus (HCV) is one of the main causes of liver-related morbidity and mortality. The virus establishes a persistent liver infection, leading to the development of chronic hepatitis, liver cirrhosis, and hepatocellular carcinomas. However, a highly effective anti-HCV drug has yet to be developed, due in part to the lack of detailed information about the HCV life cycle.

This work was supported in part by a Grant-Aid for High Technology Research, from the Ministry of Education, Science, Sports, and Culture, Japan.

Address correspondence to H. Takaku, Department of Life and Environmental Sciences and High Technology Research Center, Chiba Institute of Technology, 2-17-1 Tsudanuma, Narashino-shi, Chiba, 275-0016, Japan. E-mail: hiroshi.takaku@it-chiba.ac.jp

While aiming to develop an alternative treatment to interferons and focusing on gene therapy, we adopted a method of using RNA interference (RNAi) based on short hairpin RNA (shRNA), which is expected to yield good treatment effects as a therapeutic gene. As the target sequence, we selected the HCV core protein gene.[1–4] Conservation of the core protein sequence is extremely high among HCV genes. Because HCV functions as an mRNA and has a single strand genomic RNA, it is expected that cleavage of the core protein mRNA will inhibit nuclear transport and virus duplication.[5] We designed three shRNAs against the following regions of the HCV core protein sequence: 452 to 472 nt, 479 to 499 nt, and 503 to 523 nt. We designed shRNA expression vectors targeting the core protein site and compared their inhibitory effects.

MATERIALS AND METHODS

Plasmid Constructs

We designed DNA-based vectors expressing shRNA. Sense and antisense strands of shRNA oligonucleotides were synthesized and then annealed at 95°C for 3 min, followed by slow cooling in phosphate buffered saline (pH 7.4, containing 50 mM NaCl). These oligonucleotides contained the loop CCACACC sequence. The annealed oligonucleotides were designed to have KpnI and BamHI ends and these ends were inserted into the pU6 vector, which is based on pSV2-neo. A PolIII-type promoter was used for shRNA expression. The constructed plasmids, pU6-core-shRNA-452, pU6-core-shRNA-479, or pU6-core-shRNA-503, were used in the experiments. The plasmids pU6-core-shRNA-452, pU6-core-shRNA-479, and pU6-core-shRNA-503 were named to correspond with their respective targets in the HCV core protein regions (452–472 nt, 479–499 nt, and 503–523 nt, respectively). Scrambled shRNA (control) cloned into the same vector was used as a negative control in all experiments. The inhibitory effects of the three shRNAs were compared using a cell line produced by transducing the core protein expression vector (pEF1-core) into Huh-7 cells.

Fluorescence Microscopy

To determine the intracellular localization of the transfected shRNA expression vectors, Huh-7 cells (2×10^4 cells) were singly transfected or cotransfected with pGFP-core (nuclear exporting vector), pDsRed-PA28γ, and core-shRNA expression (pU6 plasmid) vectors, using the FuGENE 6 reagent according to the manufacturer's protocol, and were cultured for 48 h at 37°C in a 5% carbon dioxide atomosphere. Fluorescent cells were examined with a confocal microscope (Zeiss LSM5 PASCAL; Carl Zeiss, Jena,

Germany) at excitation wavelengths of 543 nm and 488 nm, using a 40× objective. Images were acquired at a 512 × 512 resolution.

Chemiluminescent Enzyme Immunoassay

We determined the efficacy of HCV core protein inhibition with the pEF1-core protein vector (0.5 μg) transfected into Huh-7 cells. pEF1-core protein vector (0.5 μg) and pU6-core shRNA (2 μg) were co-transfected into Huh-7 cells using the FuGENE 6 transfection reagent. After 48 h, intracellular HCV core protein was measured using an HCV core protein antigen chemiluminescent enzyme immunoassay (CLEIA) assay. HCV core protein

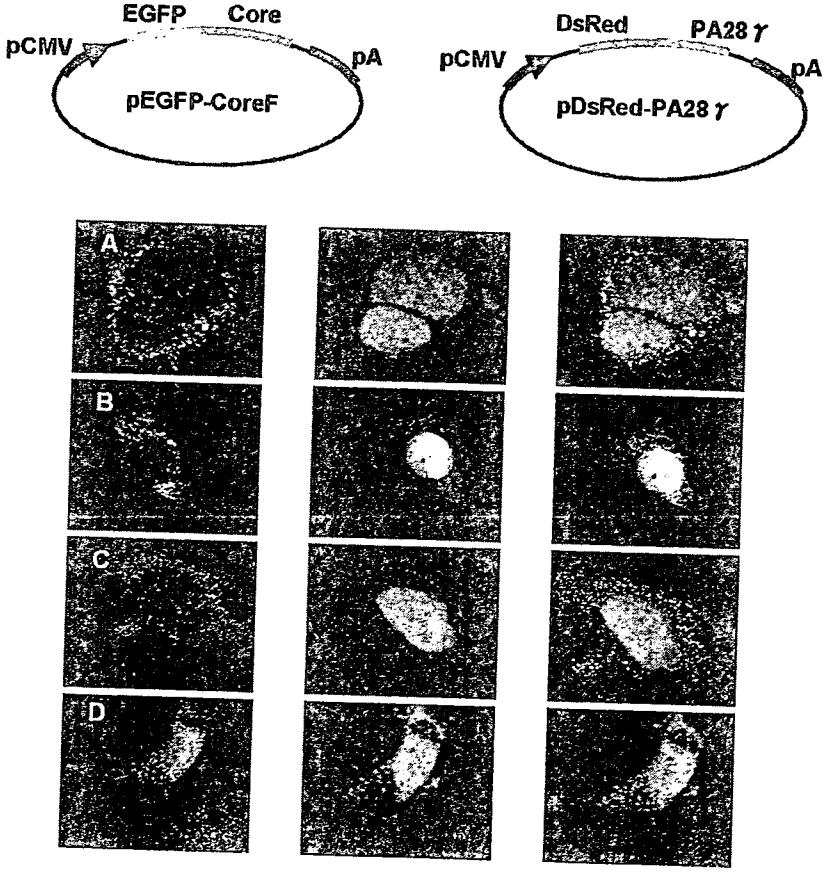

FIGURE 1 Intracellular localization of triple-transfected expression vectors in Huh-7 cells. Plate-A: Triple transfection of pU6-shRNA-452, pGFP-core (nuclear exporting vector), and pDsRed-PA28γ vectors into Huh-7 cells. Cleavage of the GFP-core protein mRNA, which is the target of shRNA-452, generated expression only in the cytosol in the GFP image, while both the DsRed and merged images show nuclear expression. Plate-B: Triple transfection of the pU6-shRNA-479, pGFP-core, and pDsRed-PA28γ vectors into Huh-7 cells. Cleavage of GFP-core protein mRNA, which is the target of shRNA-479, generated expression only in the cytosol in the GFP image, while both the DsRed and the merged images show nuclear expression. Plate-C: In a similar fashion, pU6-shRNA-503, together with pDsRed-PA28γ and pGFP-core mRNA, expressed exhibited cytoplasmic localization in the GFP image. Plate-D: The scrambled version of all of the pU6-shRNAs was transfected with the pDsRed-PA28γ and pGFP-core vectors. Nuclear expression is shown in the GFP, DsRed, and merged images.

antigen levels were determined using a fully automated CLEIA system according to the manufacturer's procedure.

RT-PCR

To determine the efficacy of pU6-shRNA-mediated gene silencing, the vectors were transiently transfected into HCV core protein-expressing Huh-7 cells (4×10^4) using the FuGENE 6 transfection reagent according to the manufacturer's protocol.

The mRNA content was assessed by reverse transcriptase-polymerase chain reaction (RT-PCR) at 48 h post-transfection and related to the amount produced in the absence of pU6-shRNA.

RESULTS AND DISCUSSION

The expression of shRNAs targeting specific portions of the HCV core protein in core protein-expressing Huh-7 cells is a critical factor for effective silencing. We confirmed the inhibitory effect of the shRNA in the cells using fluorescence microscopy. The pGFP-core, pDsRed-PA28γ, and shRNA expression vectors were simultaneously inserted into Huh-7 cells and the localization of the GFP-core was assessed by fluorescence microscopy after a 48 h culture. The core proteins were localized in the cytoplasm of the core protein-shRNA (core-shRNA-452, 479, and 503)-expressing Huh-7 cells. In

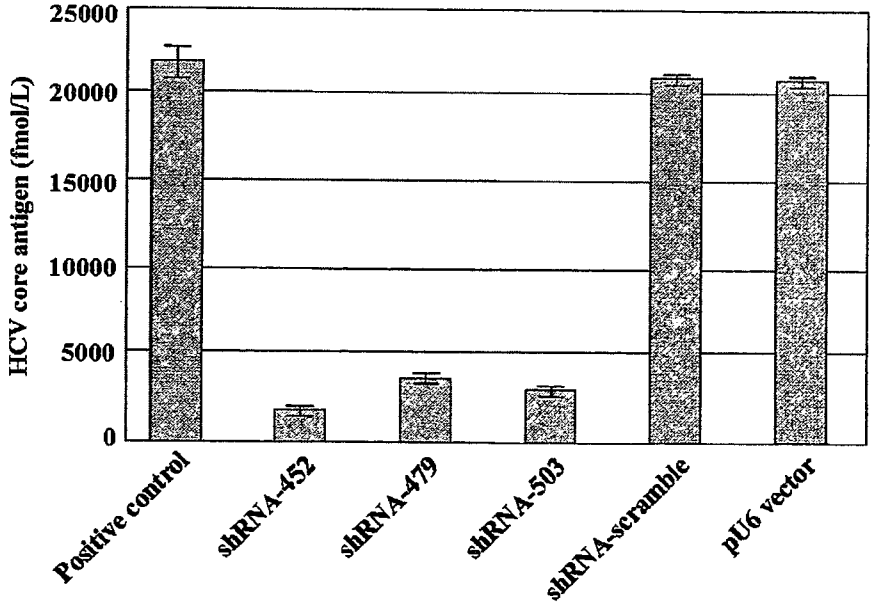

FIGURE 2 Inhibition of HCV replication by core protein-shRNAs in Huh-7 cells. The pEF1-core vector (0.5 μg) and the pU6-core-shRNAs (2 μg) were co-transfected into Huh-7 cells (4×10^4). After 48 h, the amount of intracellular HCV core protein was measured using the HCV core protein antigen CLEIA assay.

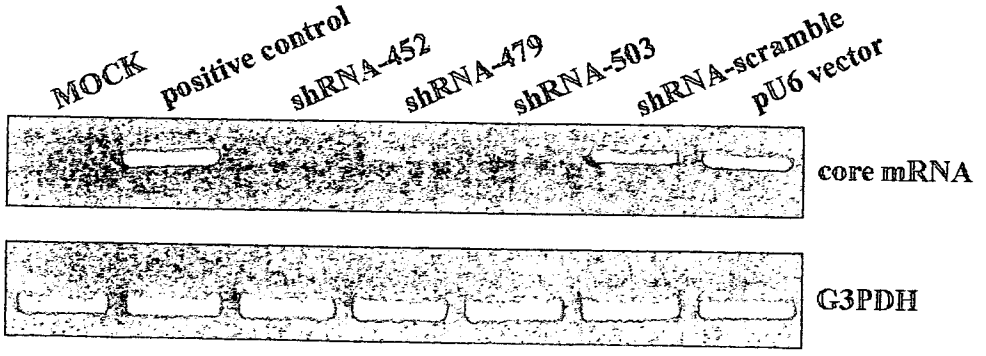

FIGURE 3 Inhibition analysis of expressed HCV core protein mRNA by shRNA expression vectors using an RT-PCR assay. The pEF1-core vector (0.5 μg) and pU6-core-shRNAs (2 μg) were co-transfected into Huh-7 cells (4×10^4). After 48 h, total RNAs were extracted and subjected to RT-PCR.

the control cells (shRNA-scramble), the core proteins were localized in the nucleus (Figure 1). This result indicates that the core protein-shRNA inhibited the expression of the core proteins.

The inhibition of core protein production was then evaluated by CLEIA, to determine whether the core proteins actually existed. The pEF1-core and each of the shRNA expression vectors were co-transfected into Huh-7 cells, and the cells were lysed and analyzed 48 h later. The results revealed that core-shRNA-452, core-shRNA-479, and core-shRNA-503 inhibited the expression of the HCV core protein (Figure 2). The inhibition mediated by the core-shRNA-452 was much stronger than that of either core-shRNA-479 or 503. In addition, the intracellular HCV core protein mRNA levels were determined by RT-PCR. The pEF1-core and each of the shRNA expression vectors were co-transfected into Huh-7 cells. The presence of the HCV core protein mRNA in the Huh-7 cells was examined by RT-PCR 48 h post-transfection. The shRNAs suppressed the expression of the core protein mRNA (Figure 3). Our study demonstrates that direct sequence-specific degradation mediated by shRNA expression in the core protein-expressing Huh-7 cells downregulates HCV core protein. Based on these results, shRNA expression vectors targeted to the core region might be useful as anti-HCV agents.

The results from this study support the potential use of shRNA expression vectors as a gene therapy approach to HCV replication, which might prove to be a valuable means of treating HCV infections.

REFERENCES

1. Yokota, T.; Sakamoto, N.; Enomoto, N.; Tanabe, Y.; Miyagishi, M.; Maekawa, S.; Yi, L.; Kurosaki, M.; Taira, K.; Watanabe, M.; Mizusawa, H.Inhibition of intracellular hepatitis C virus replication by synthetic and vector-derived small interfering RNAs. *EMBO Reports*, **2003**, 4, 1–7.
2. Wilson, J.A.; Jayasena, S.; Khvorova, A.; Sabatinos, S.; Rodrigue-Gervais, I.G.; Arya, S.; Sarangi, F.; Harris-Brandts, M.; Beaulieu, S.; Richardson, C.D. RNA interference blocks gene expression and

RNA synthesis from hepatitis C replicons propagated in human liver cells. *Proc. National Academy of Sciences of the United States of America*, **2003**, 100, 2783–2788.

3. Sorensen, D.R.; Leirdal, M.; Sioud, M. Gene silencing by systemic delivery of synthetic siRNAs in adult mice. *J. Molecular Biol.* **2003**, 327, 761–766.
4. Randall, G.; Grakoui, A.; Rice C.M. Clearance of replicating hepatitis C virus replicon RNAs in cell culture by small interfering RNAs. *Proc. National Academy of Sciences of the United States of America*, **2003**, 100, 235–240.
5. Moriishi, K.; Okabayashi, T.; Nakai, K.; Moriya, K.; Koike, K.; Murata, S.; Chiba, T.; Tanaka, K.; Suzuki, R.; Suzuki, T.; Miyamura, T.; Matsuura, Y. Proteasome activator PA28-dependent nuclear retention and degradation of hepatitis C virus core protein. *J. Virology*, **2003** 77, 10237–10249.

Nucleosides, Nucleotides, and Nucleic Acids, 26:805–808, 2007

ISSN: 1525-7770 print / 1532-2335 online
DOI: 10.1080/15257770701503647

Taylor & Francis
Taylor & Francis Group

LACK OF INTERFERON (IFN) RESPONSE TO T7 TRANSCRIBED pppG (n)(n = 2,3)-shRNA

Takuma Gondai, Kazuya Yamaguchi, and Kahoko Hashimoto □ *Department of Life and Environmental Science, Chiba Institute of Technology, Tsudanuma, Narashino-shi, Chiba, Japan*

Naoko Miyano-Kurosaki and Hiroshi Takaku □ *Department of Life and Environmental Science and High Technology Research Center, Chiba Institute of Technology, Tsudanuma, Narashino-shi, Chiba, Japan*

□ *RNA interference (RNAi) mediated by siRNAs has proved to be a highly effective gene silencing mechanism with great potential for gene therapeutic applications. However, siRNA agents have been shown to exert non-target-related biological effects and toxicities, including immune stimulation. Specifically, siRNA synthesized from a T7 RNA polymerase system can trigger the potent induction of type I IFN in a variety of cells. The single-stranded RNA can also stimulate innate cytokine responses in mammals. We found that pppGn (n = 1–3), associated with the 5′ end of the shRNA produced from the T7 RNA polymerase system, did not induce detectable levels of IFN. The residual amount of G associated with the 5′-end of the transcript was proportional to the reduction of the interferon response. We describe a T7 pppGn (n = 1–3) shRNA synthesis system that alleviates the IFN response, which will facilitate the design of siRNAs while maintaining their full efficacy.*

Keywords RNAi; shRNA; T7 RNA polymerase; type I interferon

INTRODUCTION

RNAi is a newly described natural biological phenomenon mediated by siRNA molecules, which target specific mRNAs for degradation by cellular enzymes. Surprisingly, recent studies have indicated that siRNAs can induce global upregulation of the expression of IFN-stimulated genes.[1–5] This

This work was supported by a grant-in-aid for High Technology Research (HTR) from the Ministry of Education, Science, Sports, and Culture, Japan, and by a grant-in-aid for AIDS research from the Ministry of Health, Labor, and Welfare, Japan (H17-AIDS-002).

Abbreviations: siRNA, small interfering RNA; shRNA, short hairpin RNA; TLR, Toll-like receptor; luc, luciferase; DLR™, dual-luciferase reporter; HeLa CD4$^+$ cells, HeLa cells transfected with human CD4.

Address correspondence to H.Takaku, Department of Life and Environmental Science and High Technology Research Center, Chiba Institute of Technology, 2-17-1 Tsudanuma, Narashino-shi, Chiba 275-0016, Japan. E-mail: hiroshi.takaku@it-chiba.ac.jp

effect was detected with synthetic siRNAs that were transfected into cells and with siRNAs that were produced within cells by the expression of shRNAs. Both of these studies documented significant nonspecific changes in gene expression as a consequence of the delivery of siRNAs. Two recent studies have indicated that the mechanism of the IFN response might include the recognition of the siRNAs by TLR3.[4,6] In addition, long dsRNA and single-stranded (ss) RNA of ssRNA viruses are detected through TLR7 and TLR8,[7,8] located in the endosomal membrane.[9] Recently, Kim et al.[10] showed that siRNAs synthesized using the T7 RNA polymerase system can trigger the potent induction of IFN-α and -ß in a variety of cells. The mediators of this response revealed that an initiating 5′-triphosphate was required for IFN induction.

In this study, we describe the absence of interferon induction by an new type of shRNAs, pppGG-shRNA, synthesized by bacteriophage polymerase.

RESULTS AND DISCUSSION

To investigate the RNAi-mediated silencing of luciferase activity, we initially synthesized six shRNAs targeting the luciferase gene transcript, using T7 RNA polymerase. The locations of these targets are provided in Figure 1. The luc-shRNAs include the 5′-pppGG sequence, because efficient T7 RNA polymerase initiation requires G as the first and second nts of each RNA. The inhibition of luciferase activity was measured by the DLR™ assay system. In the DLR™ assay, the firefly and Renilla luciferase activities are measured sequentially from a single sample. To determine whether pppGG-luc-shRNAs can specifically inhibit luciferase gene expression, HeLa $CD4^+$ cells were transfected with the pppGG-luc-shRNAs corresponding to the luciferase gene, and then were further transfected with pGL3-control (Firefly) and phRG-TK (Renilla). The six pppGG-luc-shRNAs (luc-1–6) all inhibited the luciferase activities (data not shown), with luc-3 and 4 showing the most inhibitory activity.

Recently, Kim et al.[10] showed that siRNAs synthesized using the T7 RNA polymerase system can trigger the potent induction of IFN-α and -ß in a variety of cells. The mediators of this response revealed that an initiating 5′-triphosphate was required for IFN induction. To verify the induction of INF by pppGG-shRNA, we designed pppGn (n = 0–3) associated with the 5′ end of shRNA-luc-3, which was transcribed by T7 RNA polymerase

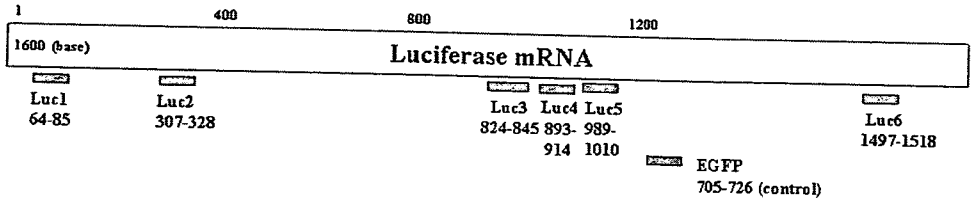

FIGURE 1 Locations of shRNAs targeting luciferase mRNA.

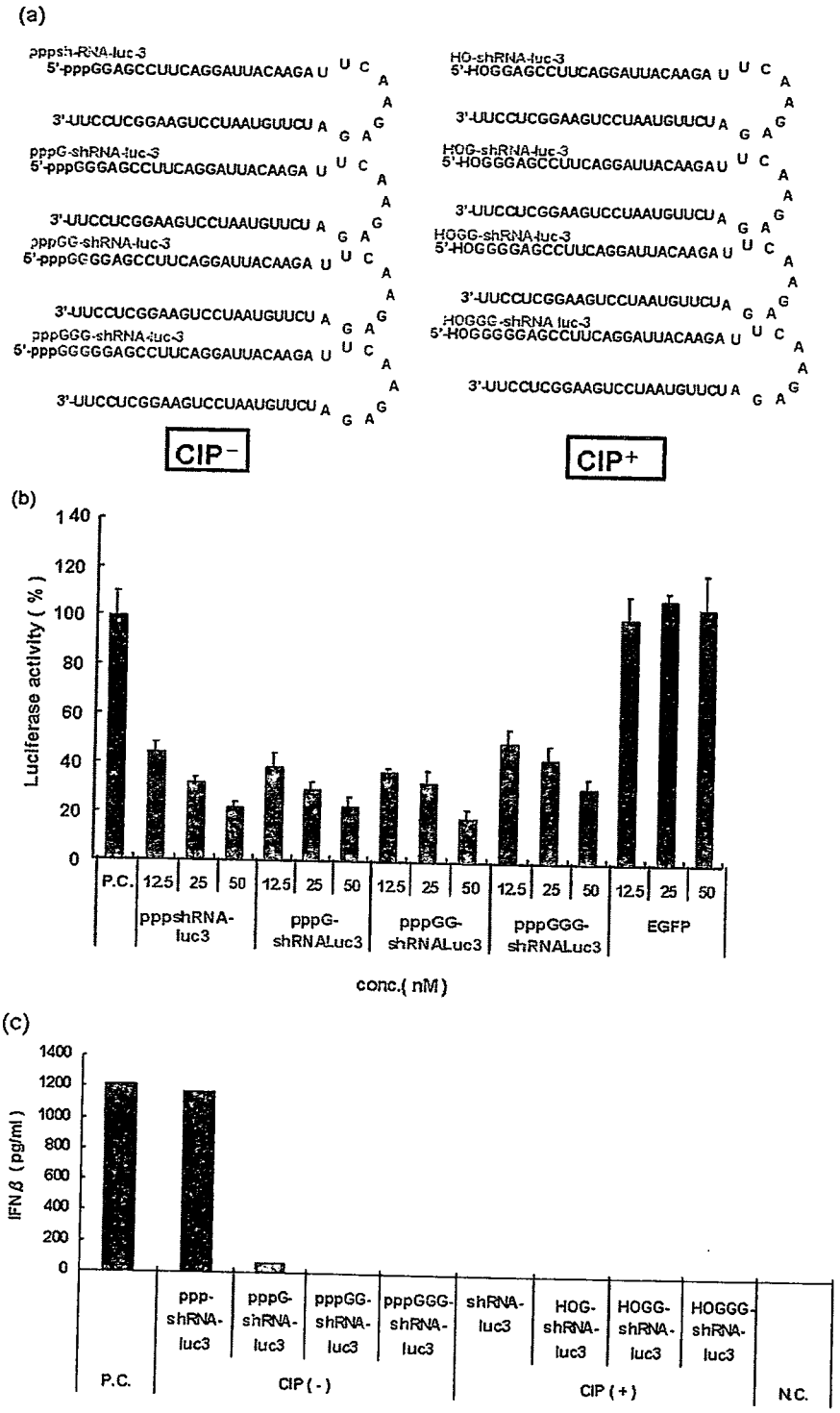

FIGURE 2 Lack of interferon induction by T7-transcribed shRNA. (a) The shRNA-luc constructs synthesized in these studies. We designed the pppGn (n = 0–3) associated with the 5′ end of the shRNA, which was transcribed by T7 RNA polymerase. We also designed the 5′-HOGn (n = 0–3) with the 5′ end of shRNA (removal of triphosphate by CIP). (b) The anti-luciferase activity of the pppGn (n = 0–3) associated with the 5′ end of shRNA-luc-3 in HeLaCD4$^+$ cells. Firefly and Renilla luciferase activities were measured consecutively by using dual-luciferase assays (Promega) 48 h after transfection. (c) The residual amount of G associated with the 5′-end of the transcript is essential for the lack of interferon induction. HeLaCD4$^+$ cells were transfected with 100 nM of pppGn (n = 0–3)-shRNAs or HOGn (n = 0–3)-shRNAs. The induced levels of IFN-β were determined by an ELISA.

(Figure 2a). The luc-3 construct induced the inhibition of luciferase activity in a dose-responsive manner (Figure 2b). However, the control pppGG-shRNA, targeting EGFP itself, showed no inhibitory effect on the luciferase activity (Figure 2b). Furthermore, the residual amount of G associated with the 5′-end of the transcript did not affect the inhibition of the luciferase activity. On the other hand, we also designed the 5′-HOGn (n = 0–3) at the 5′ end of the shRNA and tested these shRNA for IFN induction (Figure 2a). We assayed the media from pppGn or 5′-HOGn (n = 0–3)-shRNA transfected HeLa $CD4^+$ cells for IFN-ß, using an enzyme-linked immunosorbent assay (ELISA). Interferon assays from the pppGn (n = 2,3) associated with 5′ end of shRNA revealed no interferon induction in HeLa $CD4^+$cells (Figure 2c). The interferon response was initiated slightly by the pppGn (n = 1) associated with the 5′ end of the shRNA. The pppGn (n = 0) associated with the 5′ end of the shRNA showed more potent IFN induction than the pppGn (n = 1) associated with the 5′ end of the shRNA. However, no IFN induction in HeLa $CD4^+$ cells was elicited by the 5′-HOGn (n = 1–3) (Figure 2c). Furthermore, the inhibition of luciferase activity by pppGn(n = 0)-luc-shRNA observed in our data (Figure 2b-c) could be partly due to IFN induction. These results suggest that the residual amount of G associated with the 5′-end of the transcript was proportional to the reduction of the IFN response.

REFERENCES

1. Bridge, A.J.; Pebernard, S.; Ducraux, A.; Nicoulaz, A.L.; Iggo, R. Induction of an interferon response by RNAi vectors in mammalian cells. *Nature Genetics* **2003**, 34, 263–264.
2. Jackson, A.L.; Bartz, S.R.; Schelter, J.; Kobayashi, S.V.; Burchard, J.; Mao, M.; Li, B.; Cavet, G.; Linsley, P.S. Expression profiling reveals off-target gene regulation by RNAi. *Nature Biotechnol.* **2003**, 21, 635–637.
3. Sledz, C.A.; Holko, M.; de Veer, M.J.; Silverman, R.H.; Williams, B.R. Activation of the interferon system by short-interfering RNAs. *Nature Cell Biol.* **2003**, 9, 834–839 .
4. Kariko, K.; Bhuyan, P.; Capodici, J.; Weissman, D. Small interfering RNAs mediate sequence-independent gene suppression and induce immune activation by signaling through toll-like receptor 3. *J. Immunol.* **2004**, 172, 6545–6549.
5. Persengiev, S.P.; Zhu, X.; Green, M.R. Nonspecific, concentration-dependent stimulation and repression of mammalian gene expression by small interfering RNAs (siRNAs). *RNA* **2004**, 10, 12–18.
6. Heidel, J.D.; Hu, S.; Liu, X.F.; Triche, T.J.; Davis, M.E. Lack of interferon response in animals to naked siRNAs. *Nature Biotechnol.* **2004**, 22, 1579–1582.
7. Diebold, S.S.; Kaisho, T.; Hemmi, H.; Akira, S.; Reise-Sousa, C. Innate antiviral responses by means of TLR7-mediated recognition of single-stranded RNA. *Science* **2004**, 303, 1529–1531.
8. Heil, F.; Ahmad-Nejad, P.; Hemmi, H.; Hochrein, H.; Ampenberger, F.; Gellert, T.; Dietrich, H.; Lipford, G.; Takeda, K.; Akira, S.; Wagner, H.; Bauer, S. The Toll-like receptor 7 (TLR7)-specific stimulus loxoribine uncovers a strong relationship within the TLR7, 8 and 9 subfamily. *European J. Immunol.* **2003**, 33, 2987–2997.
9. Heil, F.; Hemmi, H.; Hochrein, H.; Ampenberger, F.; Kirschning, C.; Akira, S.; Lipford, G.; Wagner, H.; Bauer S. Species-specific recognition of single-stranded RNA via toll-like receptor 7 and 8. *Science* **2004**, 303, 1481–1482.
10. Kim, D.H.; Longo, M.; Han, Y.; Lundberg, P.; Cantin, E.; Rossi, J.J. Interferon induction by siRNAs and ssRNAs synthesized by phage polymerase. *Nature Biotechnol.* **2004**, 22, 321–325.

Available online at www.sciencedirect.com
ScienceDirect
Biochemical and Biophysical Research Communications 360 (2007) 115–121
BBRC
www.elsevier.com/locate/ybbrc

PKC412 (CGP41251) modulates the proliferation and lipopolysaccharide-induced inflammatory responses of RAW 264.7 macrophages

Katsutoshi Miyatake [a,b], Hiroshi Inoue [b,*], Kahoko Hashimoto [c], Hiroshi Takaku [c], Yoichiro Takata [a], Shunji Nakano [a], Natsuo Yasui [a], Mitsuo Itakura [b]

[a] *Department of Orthopedics, Institute of Health Biosciences, The University of Tokushima Graduate School, Tokushima, Japan*
[b] *Institute for Genome Research, The University of Tokushima, Tokushima, Japan*
[c] *Department of Life and Environmental Sciences, Faculty of Engineering, Chiba Institute of Technology, Chiba, Japan*

Received 15 May 2007
Available online 12 June 2007

Abstract

PKC412 (CGP41251) is a multitarget protein kinase inhibitor with anti-tumor activities. Here, we investigated the effects of PKC412 on macrophages. PKC412 inhibited the proliferation of murine RAW 264.7 macrophages through induction of G2/M cell cycle arrest and apoptosis. At non-toxic drug concentrations, PKC412 significantly suppressed the lipopolysaccharide (LPS)-induced release of TNF-α and nitric oxide, while instead enhancing IL-6 secretion. PKC412 attenuated LPS-induced phosphorylations of MKK4 and JNK, as well as AP-1 DNA binding activities. Furthermore, PKC412 suppressed LPS-induced Akt and GSK-3β phosphorylations. These results suggest that the anti-proliferative and immunomodulatory effects of PKC412 are, at least in part, mediated through its interference with the MKK4/JNK/AP-1 and/or Akt/GSK-3β pathways. Since macrophages contribute significantly to the development of both acute and chronic inflammation, PKC412 may have therapeutic potential and applications in treating inflammatory and/or autoimmune diseases.

Keywords: PKC412; RAW 264.7 macrophage; Lipopolysaccharide; TNF-α; IL-6; Nitric oxide

PKC412 (CGP41251), a derivative of the naturally occurring alkaloid staurosporine, was originally identified as a selective inhibitor of the conventional (α, β, and γ) and novel (δ, ε, and η) isoforms of protein kinase C (PKC), and was subsequently shown to inhibit a variety of tyrosine kinases including FLT3, PDGF-α and -β receptors, and the c-kit receptor [1]. Because of its potential to inhibit growth, angiogenesis and P-glycoprotein-mediated multidrug resistance in tumor cells, PKC412 is being developed as a therapeutic agent. Indeed, there is strong preclinical evidence that PKC412, alone or in combination with other anti-cancer agents, can inhibit tumor growth [1,2]. Furthermore, results of phase I/II clinical trials of PKC412 have shown that this orally available agent effectively suppresses cancer cell proliferation, and is relatively safe with minimal toxicity [3–5].

While the kinases inhibited by PKC412 play key roles in cell proliferation and tumorigenesis, they have also been implicated in other cellular processes such as immune responses and neuronal function. For example, several isoforms of PKC are activated by antigen receptors in T- and B-lymphocytes, coupling to signal transduction pathways that regulate their migration, differentiation, and proliferation [6]. Hence, it is reasonable to speculate that PKC412 may potently modulate the activity of lymphocytes and other immune cells, and thus possibly being effective for treating immune-mediated disorders. In fact, a recent study showed that PKC412 effectively inhibits normal human

* Corresponding author. Fax: +81 88 633 9484.
E-mail address: hinoue@genome.tokushima-u.ac.jp (H. Inoue).

0006-291X/$ - see front matter © 2007 Published by Elsevier Inc.
doi:10.1016/j.bbrc.2007.06.009

T-cell activation, proliferation and TNF-α production in response to mitogenic lectins [7].

Macrophages synthesize a wide variety of immunomodulatory mediators including proinflammatory cytokines and nitric oxide (NO), and serve as an essential interface between innate and adaptive immunity [8]. Their dysregulated activities contribute to the pathogenesis of many chronic inflammatory diseases such as rheumatoid arthritis (RA) and inflammatory bowel disease. In the case of RA, a prominent macrophage infiltrate is commonly found in the inflamed synovial tissues [9]. These cells usually display signs of activation and exhibit widespread proinflammatory, destructive and remodeling capabilities, contributing to both acute and chronic phases of inflammation. Consequently, a number of approaches designed to counter macrophage activities have substantially improved RA treatment [9]. In the present study, we investigated whether PKC412 can modulate macrophage proliferation and production of TNF-α, IL-6 and NO, using murine RAW 264.7 macrophages.

Materials and methods

Reagents and cell culture. PKC412 (CGP41251/4′-*N*-benzoyl staurosporine) was obtained from LC Laboratories, and stored at −80 °C as a 10 mM stock solution in dimethyl-formamide. Lipopolysaccharide (LPS) from *Escherichia coli* O55:B5 was obtained from Calbiochem. All other reagents were of analytical grade, and were purchased from Sigma. RAW 264.7 macrophages were cultured at 37 °C under 5% CO_2 in RPMI1640 (Invitrogen) containing 10% FBS and antibiotics.

Cytotoxicity and proliferation assays. Cells were seeded at a density of 1×10^4 cells/well in a 96-well plate. The next day, the cells were incubated with various concentrations of PKC412 (0.01–10 μM) for 24, 48 or 72 h, and cell viability was determined thereafter using a colorimetric MTT test (Cell Proliferation Kit I; Roche). The rates of DNA synthesis were measured quantitatively using a BrdU Cell Proliferation Kit (Roche). The 50% inhibitory concentration (IC_{50}, MTT assay) and 50% effective concentration (EC_{50}, BrdU assay) were calculated graphically using a curve-fitting function of the Excel 2003 (Microsoft) software.

Morphological assessment and DNA fragmentation assay. Cells (5×10^5 cells/10-cm dish) were treated with 0.1–2.5 μM of PKC412 for 12 h, and were morphologically assessed by light microscopy, and by fluorescence microscopy using the standard Acridine orange-ethidium bromide (AO–EB) double staining procedure. For DNA fragmentation assay, cellular DNA was isolated by phenol/chloroform extraction and subjected to electrophoresis on EB-stained 1.5% agarose gels.

Flow-cytometric analysis. Following PKC412 treatment, the cells were harvested and fixed with 70% ethanol at −20 °C for 18 h. After washing, 1×10^6 cells were resuspended in a staining solution consisting of 0.2 mg/ml DNase-free RNase and 50 μg/ml propidium iodide (Invitrogen), and incubated for 1 h at room temperature, followed by flow-cytometric analysis using a FACSCalibur (Becton–Dickinson).

Measurement of nitrite production and quantification of cytokine concentrations. Cells were seeded in 96-well plates one day before the experiment at a density of 2×10^5 cells/well. The next day, the cells were preincubated with different concentrations of PKC412 for 1 h, followed by stimulation with 0.5 μg/ml of LPS. After 12 and 24 h, the supernatant medium was collected and the NO_2^- concentration was determined with the Griess Reagent System (Promega). The amounts of TNF-α and IL-6 released into the media were analyzed with ELISA kits (R&D Systems).

RNA isolation and RT-PCR. Total RNA was isolated using an RNeasy kit (Qiagen). First-strand cDNA was synthesized using SuperScript III Reverse Transcriptase (Invitrogen). Semi-quantitative real-time RT-PCR was performed using TaqMan Gene Expression Assays (*Tnfa*, Mm00443258_m1; *Il6*, Mm00446190_m1; *Nos2*, Mm00440485_m1; *Hprt1*, Mm01545399_m1; Applied Biosystems) on an ABI Prism 7900HT system. The comparative C_t method was used to determine the ratio of target to endogenous control gene (*Hprt1*) expression.

Immunoblotting. The primary antibodies used were anti-iNOS (Upstate Biotechnology), anti-GAPDH (Ambion), and anti-Nucleoporin p62 (Nup62; BD Biosciences), as well as antibodies from the Phospho-MAPK, MAPK Family, Phospho-SAPK/JNK and Phospho-Akt Pathway Antibody Sampler Kits (CST), and all were used at the manufacturer's recommended dilutions. Immunoblot analysis was performed according to standard procedures.

Electrophoretic mobility shift assay (EMSA). Subconfluent cells were pretreated with PKC412 for 1 h, followed by stimulation with 0.5 μg/ml of LPS for 30 min. Nuclear extracts were prepared using a Nuclear Extraction Kit (Active Motif), and EMSA was performed using Gel Shift Assay Systems (Promega). Briefly, 1 μg of the nuclear extracts was mixed with 20 pmol of the appropriate [^{32}P]-labeled oligonucleotides (AP-1, NF-κB), then incubated for 30 min at room temperature, and resolved on a 4% polyacrylamide gel, transferred to filter paper, and visualized by autoradiography.

Statistical analysis. The results are presented as means ± SD of four to six samples. Differences between two groups were tested using the unpaired two-tailed Student's *t* test, and $P < 0.05$ was considered to represent a statistically significant difference.

Results

PKC412 inhibits proliferation of RAW 264.7 macrophages through induction of G2/M cell cycle arrest and apoptosis

In the MTT assay, exposure of RAW 264.7 macrophages to 0.01–10 μM PKC412 resulted in a dose- and time-dependent reduction in cell viability (Fig. 1A). The effective PKC412 concentrations for 50% inhibition (IC_{50}) of RAW 264.7 cell growth after 24, 48, and 72 h were 3.82, 1.15, and 0.95 μM, respectively. PKC412 at concentrations below 0.1 μM had no growth inhibitory effect. The DNA synthesis rate measured by BrdU incorporation assay confirmed the anti-proliferative effect of PKC412 (EC_{50}/24 h = 2.67 μM; Supplementary Fig. S1).

Microscopic examination of PKC412-treated RAW 264.7 cells revealed dramatic morphological alterations including irregular shape, heterogeneous size and occasional long projections (Fig. S2A). The AO-EB staining showed changes characteristic of apoptosis (Fig. S2B). As shown in Fig. 1B, the formation of DNA nucleosome ladders was clearly detected in cells treated with 2.5 μM PKC412 for 12 h, while a very faint apoptotic ladder/smear pattern was visible in cells treated with 1.0 μM PKC412. Cell cycle analysis revealed that treatment with PKC412 increased the proportion of cells in the G2/M and sub-G1 (apoptotic cells) phases of the cell cycle in a time-dependent manner, with a corresponding decrease in the numbers of cells in the G0/G1 and S phases (Fig. 1C).

PKC412 differentially modulates the inflammatory response of RAW 264.7 macrophages to LPS

To examine whether PKC412 affects LPS-stimulated productions of TNF-α and IL-6 from RAW 264.7 cells,

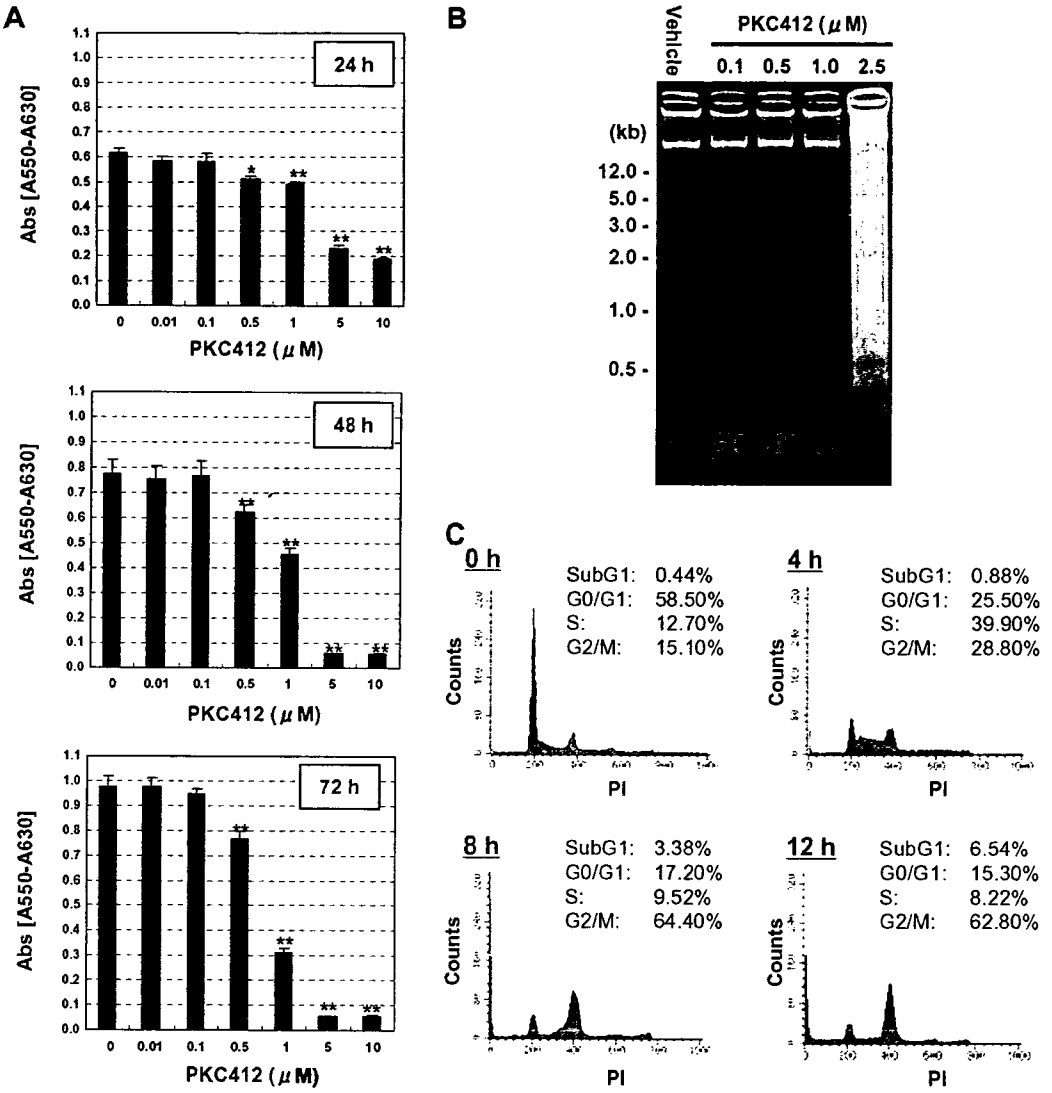

Fig. 1. Effects of PKC412 on RAW 264.7 macrophage viability (A) MTT assay. Cells were treated with increasing concentrations of PKC412 (0–10 μM) for 24, 48 or 72 h. Each bar represents the mean absorbance values (A_{570}–A_{630}) ± SD of four to six determinations. Note that absorbance values are directly proportional to cell viability, and are increased in a time-dependent manner in vehicle-treated cells. $^{*}P < 0.001$, $^{**}P < 0.0001$ versus vehicle-treated control cells (unpaired t-test). (B) DNA fragmentation assay. Cells were treated with various concentrations of PKC412 (0–2.5 μM) for 12 h. Genomic DNA was separated on an agarose gel and stained with EB. (C) RAW 264.7 cells were treated with 2.5 μM PKC412 for 4, 8, and 12 h, stained with PI, and the cell cycle distribution was then analyzed by flow cytometry. Representative histograms at each time point of at least three independent experiments are shown.

PKC412 drug concentrations (0.02–0.5 μM) and exposure times (12 or 24 h) were chosen to minimize the influence of its inhibitory effects on cell viability. A 12 h incubation of cells with 0.5 μg/ml of LPS caused a marked increase in TNF-α production as compared to non-stimulated cells (49.8 ± 5.7 versus 0.04 ± 0.06 ng/ml; Fig. 2A), and it was significantly reduced by PKC412 in a dose-dependent manner. Following 24 h LPS-stimulation, there was a decline in LPS-stimulated TNF-α levels in both vehicle- and PKC412-treated cells. This phenomenon has been described in previous reports [10,11], and is presumably attributable to uncharacterized clearance mechanisms (e.g. increased degradation and/or internalization). At this time point, the difference became less clear but a persistent inhibitory effect of PKC412 was observed. In contrast to TNF-α, no significant effects of PKC412 were found in LPS-stimulated IL-6 secretion after a 12 h incubation period (Fig. 2B). In fact, after a 24 h culture, IL-6 production was significantly enhanced by PKC412 at a concentration of $\geqslant$0.1 μM. Basal levels of TNF-α and IL-6 were not affected by treatment with either vehicle or PKC412.

Production of NO was increased approximately 12-fold after 12 h stimulation with LPS in vehicle-treated cells, and NO production was dose-dependently reduced in PKC412-treated cells (Fig. 2C). Following 24 h stimulation with LPS, NO production was elevated in both vehicle- and

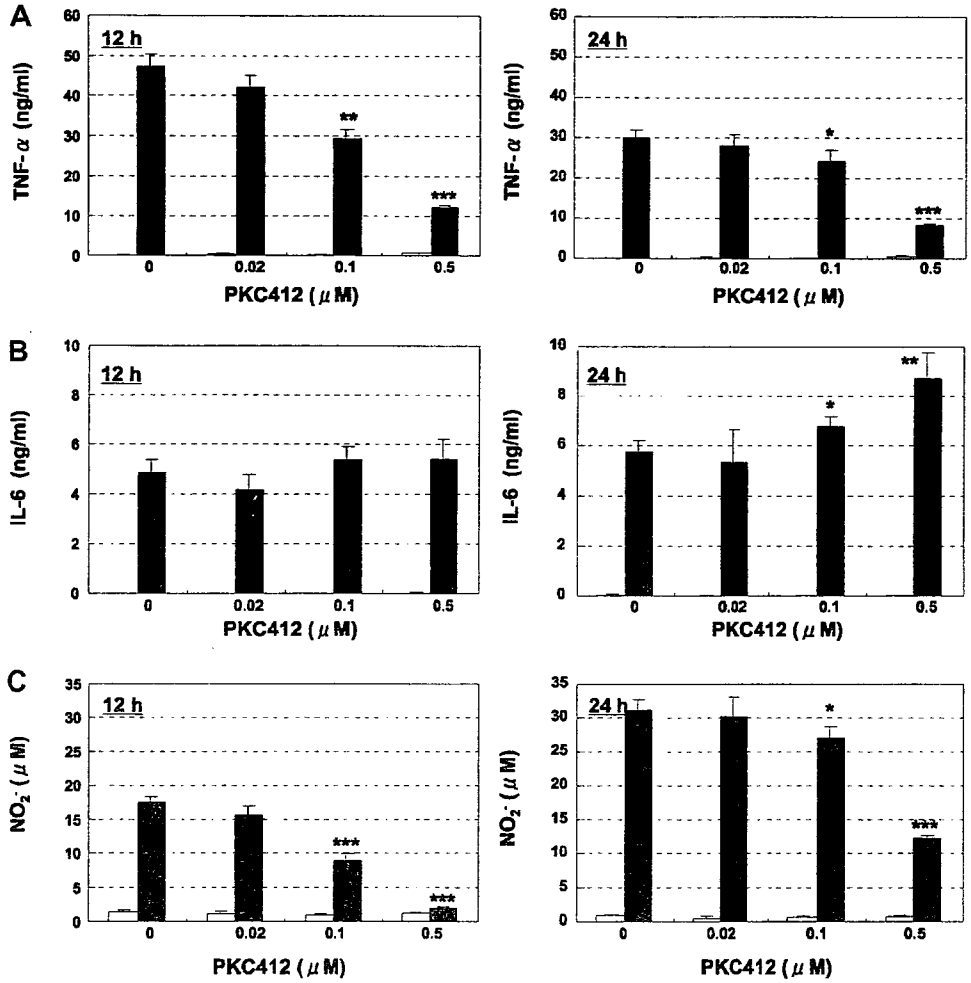

Fig. 2. Effects of PKC412 on LPS-induced inflammatory mediator production. RAW 264.7 macrophages were pretreated with various concentrations of PKC412 for 1 h, and further incubated either in the presence (black bars) or absence of 0.5 μg/ml of LPS (white bars). After 12 or 24 h incubation, the supernatant medium was collected and used to assay for TNF-α (A), IL-6 (B), and NO (C). Values are means ± SD ($n = 4$–6 in each group). Statistical significance (unpaired t-test) is based on the difference as compared to LPS-stimulated, vehicle-treated cells. $^{*}P < 0.05$, $^{**}P < 0.005$, $^{***}P < 0.0001$.

PKC412-treated cells, but persistent inhibitory effects of PKC412 were observed. Western blot analysis of iNOS protein was consistent with NO production values (Fig. S3): PKC412 significantly attenuated LPS-induced iNOS expression in a parallel concentration-dependent manner.

Effects of PKC412 on LPS-induced gene expressions

To gain greater insight into the mechanisms by which PKC412 modulates productions of TNF-α, IL-6, and NO, we examined the effects of PKC412 on the expressions of the corresponding mRNAs, *Tnfa*, *Il6*, and *Nos2* (the gene encoding murine iNOS protein) (Fig. S4). Transcripts for these genes were markedly induced following LPS stimulation, although they exhibited distinct temporal differences in peak expression levels. Specifically, the induction of *Tnfa* mRNA was the fastest, peaking at 2 h after stimulation, with mRNA levels subsequently decreasing. Strong induction of *Il6* was also observed in the relatively early period of LPS treatment: however, the induction kinetics was delayed compared to *Tnfa*, with peak values achieved at 4 h. *Nos2* expression levels demonstrated a time-dependent increase over a 24 h culture period.

At a concentration of 0.5 μM, PKC412 significantly attenuated LPS-induced *Tnfa* expression over a 24 h time course (Fig. S4A). A similar inhibitory effect of PKC412 on *Il6* expression was observed at 4 h after LPS treatment: however, following longer exposures (16–24 h), PKC412 appeared to enhance *Il6* expression as compared to the vehicle, although these differences were not statistically significant (Fig. S4B). Effects of PKC412 on LPS-induced *Nos2* expression were complex and a time-dependent biphasic effect was observed (Fig. S4C). That is, *Nos2* expression was enhanced by PKC412 at early time points (≤4 h), while later being markedly suppressed.

Effects of PKC412 on macrophage signaling pathways

Our preliminary study showed that, in RAW 264.7 cells, LPS induced rapid phosphorylation of all three MAPKs (ERK, p38, and JNK), with peak activation at approximately 15 min after stimulation (data not shown). To determine if PKC412 blocked the activation of MAPKs, cells were stimulated with LPS in the presence of PKC412 (0–2 μM). As shown in Fig. 3A, PKC412 treatment dose-dependently blocked LPS-induced JNK phosphorylation without affecting the total level of protein, whereas phosphorylations of ERK and p38 were unaffected. Activation of JNK in response to LPS may be mediated through MKK4. Once activated, JNK phosphorylates and activates c-Jun and ATF-2, the major components of AP-1 and AP-1-like transcription factors, and, in turn, controls the expression of a number of genes whose promoter regions contain AP-1 binding sites [12]. We found that PKC412 concentration-dependently attenuated the phosphorylation of MKK4 in response to LPS (Fig. 3A). The blockade of the MKK4/JNK signaling pathway by PKC412 was further confirmed because, within the same concentration range, it also inhibited the LPS-induced phosphorylation of c-Jun and, to a lesser degree, that of ATF-2 (Fig. 3B).

PKC412 also markedly inhibited LPS-stimulated phosphorylation of Akt on both Ser473 and Thr308, and its downstream molecule GSK-3β (Fig. 3C). These inhibitory effects were evident even at a low drug concentration of 0.25 μM. PDK1 is an upstream Akt kinase phosphorylating Thr308, and is activated mainly by PI3K-generated lipids [13]. We observed a high steady-state level of phosphorylated PDK1 in non-LPS-treated RAW 264.7 cells, which was only marginally suppressed by PKC412 (Fig. 3C).

Consistent with the observed inhibitory effects on MKK4/JNK/c-Jun activation, the EMSA results showed PKC412 to significantly inhibit LPS-induced AP-1 DNA binding activity (Fig. S5). LPS stimulation also resulted in a significant increase in the DNA binding activity of NF-κB in RAW 264.7 macrophages, while PKC412 had no significant effects (Fig. S5). Consistently, PKC412 had no effects on the kinetics of IκB-α and -β in response to LPS, the phosphorylation and degradation of which are responsible for the activation of NF-κB (data not shown).

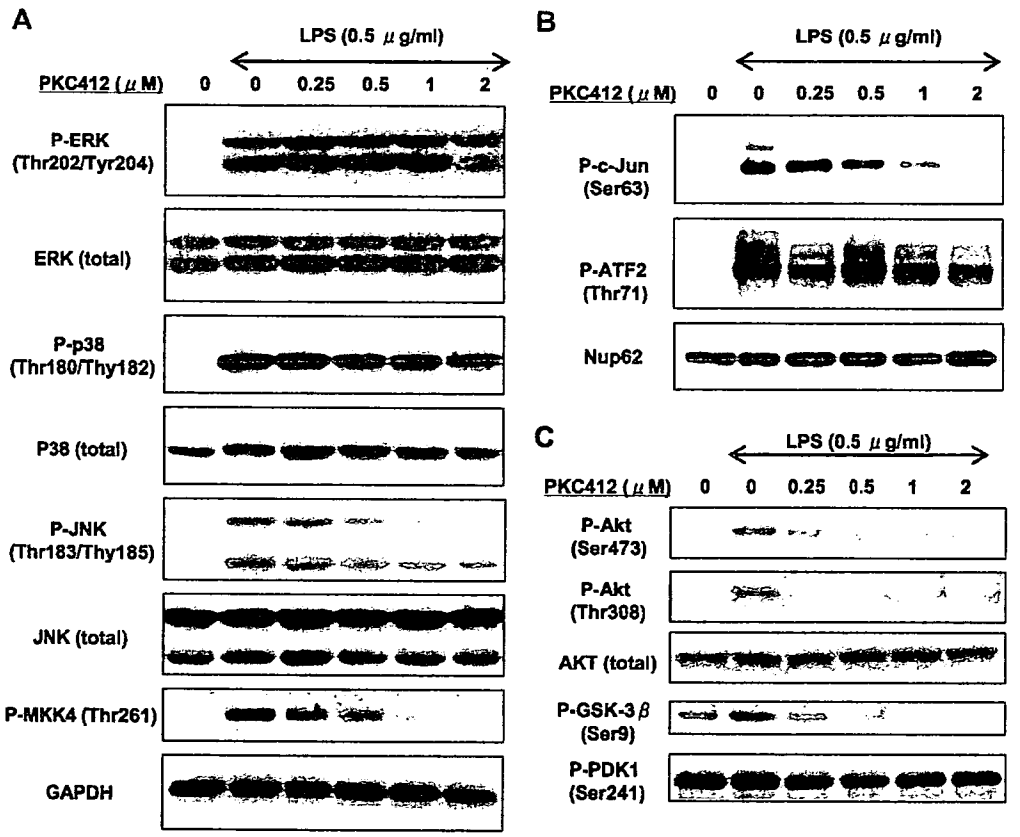

Fig. 3. Effects of PKC412 on LPS-induced signaling pathways. (A) RAW 264.7 cells were pretreated with the indicated concentrations of PKC412, followed by 15 min stimulation with LPS (0.5 μg/ml). Activations of ERK, p38, JNK and MKK4 were assessed by immunoblotting using phospho-specific anti-active antibodies. The blot was reprobed with antibodies against corresponding total-proteins and GAPDH. (B) Cells were treated with PKC412 as described above, and stimulated with LPS for 30 min. The nuclear extracts were subjected to immunoblotting using phospho-specific antibodies for c-Jun and ATF-2, and anti-Nup62 antibody (loading control). (C) Activations of Akt, GSK-3β and PDK1 were assessed using phospho-specific antibodies, and the blot was reprobed with anti-total-Akt and GAPDH antibodies.

Discussion

PKC412 inhibited cell proliferation of RAW 264.7 macrophages in a dose- and time-dependent manner, with IC_{50} values (3.82–0.95 μM for 24–72 h) slightly higher than those reported for various tumor and normal cell lines, as well as in xenograft models (approximately 0.2–1 μM). The anti-proliferative properties of PKC412 in RAW 264.7 cells were associated with induction of cell cycle arrest in the G2/M phase and apoptosis. These findings are consistent with previous studies in other cell types showing exposure of cells to PKC412 to result in an increase in the G2/M phase of the cell cycle concomitant with increased polyploidy, apoptosis and enhanced sensitivity to ionizing radiation [1].

We confirmed that non-toxic doses of PKC412 modulate inflammatory responses of RAW 264.7 macrophages. PKC412 (0.1–0.5 μM) dose-dependently inhibited LPS-induced enhancement of TNF-α and NO releases. These inhibitory effects were more significant for relatively short exposure times (12 h), and tended to diminish over longer incubation periods. This observation might relate to the biological half-life of PKC412, or might be attributable to our use of a relatively high (sub-maximal) concentration of LPS (0.5 μg/ml) for stimulation. Alternatively, an autocrine feedback mechanism might be involved, as it has been proposed that macrophage-derived TNF-α or NO can activate macrophages themselves [14,15]. In contrast to TNF-α and NO, IL-6 production was not inhibited, but rather was enhanced by PKC412 following 24 h LPS-stimulation. Previous studies have demonstrated that IL-6 exerts pro- as well as anti-inflammatory activities during acute inflammatory responses [16,17]. Therefore, how IL-6 enhancement by PKC412 is associated with the eventual outcome of LPS-induced inflammation in macrophages remains unclear.

Overall, our results on the production of inflammatory mediators are consistent with the earlier findings of Tremblay et al. [18], who treated RAW 264.7 cells with a single high dose of PKC412 (1 μM) under serum-free conditions and measured LPS-induced cytokine productions using bioassay-based methods instead of ELISA. Our experiments were conducted in the presence of serum in the medium, since, without serum, the RAW 264.7 macrophages rapidly became apoptotic (data not shown). A similar observation was reported previously, and an apoptotic mechanism involving autocrine secretion of IFN-α and -β has been suggested [19]. Yet, under our experimental conditions, it is possible that serum protein binding of PKC412 interferes with its pharmacological activity or distribution: however, it has been shown that oral administration of PKC412 at 150–300 mg/day to cancer patients resulted in steady-state PKC412 plasma levels in the micromolar range [3], suggesting that the drug concentrations used in this study are at least physiologically relevant.

Gene expression analyses revealed different temporal induction profiles for *Tnfa*, *Il6*, and *Nos2* genes with LPS stimulation. Interestingly, the effects of PKC412 on transcription levels were also variable among the genes investigated, and did not necessarily correspond to the results of production/secretion. These observations suggested that PKC412 affects macrophage production of inflammatory mediators by interfering at not only the transcriptional but also other levels, presumably translational and/or post-translational regulation.

Our results showed that PKC412 inhibited LPS-induced JNK phosphorylation and AP-1 activation in RAW 264.7 cells. As phosphorylation of MKK4 was also inhibited by PKC412, it is likely that PKC412 acts proximal to MKK4, which is regulated by a complex and inter-related group of MAPK kinase kinases (MAPKKKs). PKC412 also markedly suppressed LPS-stimulated phosphorylation of both Akt and its downstream molecule GSK-3β, yet exerted no effects on NF-κB activities, another downstream target of Akt. Although it has been well accepted that Akt is a downstream target of PI3K [13], the role of the PI3K/Akt signal pathway in LPS signaling is controversial. There are several reports describing a positive role for PI3K/Akt in LPS-induced inflammatory responses, while several others have demonstrated a negative role with special emphasis on its protective effects from prolonged inflammatory responses [20–22]. In addition, one report suggested the PI3K-independent pathway to be involved in Akt activation in LPS-stimulated RAW 264.7 cells [23]. Further studies are necessary to elucidate the significance of Akt signaling inhibition by PKC412 in relation to macrophage functions.

In summary, we have shown that PKC412 exerts both anti-proliferative/apoptosis-inducing and immunomodulatory activities in RAW 264.7 macrophages, and that these activities are likely to be mediated, at least in part, by inhibition of the MKK4/JNK/AP-1 and/or Akt/GSK-3β signaling pathways. Since macrophages contribute to both acute and chronic inflammatory diseases and their function is a potential target for novel therapeutic intervention, our results suggest that PKC412 has potential clinical utility as it can counter macrophage activities.

Acknowledgments

We thank Drs. Takeshi Nitta and Yousuke Takahama (The University of Tokushima) for their help with the FACS analysis. This study was supported by grants from the Japan Rheumatism Foundation (Tsumura Award for Clinical Medicine in Osteoarthropathy) and the Ministry of Education, Science and Technology (Knowledge Cluster Initiative).

Appendix A. Supplementary data

Supplementary data associated with this article can be found, in the online version, at doi:10.1016/j.bbrc.2007.06.009.

References

[1] D. Fabbro, S. Ruetz, S. Bodis, M. Pruschy, K. Csermak, A. Man, P. Campochiaro, J. Wood, T. O'Reilly, T. Meyer, PKC412-a protein kinase inhibitor with a broad therapeutic potential, Anticancer Drug Des. 15 (2000) 17–28.

[2] Y. Ikegami, S. Yano, K. Nakao, F. Fujita, M. Fujita, Y. Sakamoto, N. Murata, K. Isowa, Antitumor activity of the new selective protein kinase C inhibitor 4′-*N*-benzoyl staurosporine on murine and human tumor models, Arzneimittelforschung 45 (1995) 1225–1230.

[3] D.J. Propper, A.C. McDonald, A. Man, P. Thavasu, F. Balkwill, J.P. Braybrooke, F. Caponigro, P. Graf, C. Dutreix, R. Blackie, S.B. Kaye, T.S. Ganesan, D.C. Talbot, A.L. Harris, C. Twelves, Phase I and pharmacokinetic study of PKC412, an inhibitor of protein kinase C, J. Clin. Oncol. 19 (2001) 1485–1492.

[4] C. Monnerat, R. Henriksson, T. Le Chevalier, S. Novello, P. Berthaud, S. Faivre, E. Raymond, Phase I study of PKC412 (N-benzoyl-staurosporine), a novel oral protein kinase C inhibitor, combined with gemcitabine and cisplatin in patients with non-small-cell lung cancer, Ann. Oncol. 15 (2004) 316–323.

[5] R.M. Stone, D.J. DeAngelo, V. Klimek, I. Galinsky, E. Estey, S.D. Nimer, W. Grandin, D. Lebwohl, Y. Wang, P. Cohen, E.A. Fox, D. Neuberg, J. Clark, D.G. Gilliland, J.D. Griffin, Patients with acute myeloid leukemia and an activating mutation in FLT3 respond to a small-molecule FLT3 tyrosine kinase inhibitor, PKC412, Blood 105 (2005) 54–60.

[6] S.L. Tan, P.J. Parker, Emerging and diverse roles of protein kinase C in immune cell signalling, Biochem. J. 376 (2003) 545–552.

[7] M.S. Si, B.A. Reitz, D.C. Borie, Effects of the kinase inhibitor CGP41251 (PKC 412) on lymphocyte activation and TNF-alpha production, Int. Immunopharmacol. 5 (2005) 1141–1149.

[8] J.S. Duffield, The inflammatory macrophage: a story of Jekyll and Hyde, Clin. Sci. 104 (2003) 27–38.

[9] R.W. Kinne, R. Bräuer, B. Stuhlmüller, E. Palombo-Kinne, G.R. Burmester, Macrophages in rheumatoid arthritis, Arthritis Res. 2 (2000) 189–202.

[10] W.H. Watson, Y. Zhao, R.K. Chawla, *S*-Adenosylmethionine attenuates the lipopolysaccharide-induced expression of the gene for tumour necrosis factor alpha, Biochem. J. 342 (1999) 21–25.

[11] I.S. Singh, R.M. Viscardi, I. Kalvakolanu, S. Calderwood, J.D. Hasday, Inhibition of tumor necrosis factor-alpha transcription in macrophages exposed to febrile range temperature. A possible role for heat shock factor-1 as a negative transcriptional regulator, J. Biol. Chem. 275 (2000) 9841–9848.

[12] J.S. Schorey, A.M. Cooper, Macrophage signalling upon mycobacterial infection: the MAP kinases lead the way, Cell Microbiol. 5 (2003) 133–142.

[13] L.C. Cantley, The phosphoinositide 3-kinase pathway, Science 296 (2002) 1655–1657.

[14] A.R. Clemons-Miller, G.W. Cox, J. Suttles, R.D. Stout, LPS stimulation of TNF-receptor deficient macrophages: a differential role for TNF-alpha autocrine signaling in the induction of cytokine and nitric oxide production, Immunobiology 202 (2000) 477–492.

[15] J. Xaus, M. Comalada, A.F. Valledor, J. Lloberas, F. López-Soriano, J.M. Argilés, C. Bogdan, A. Celada, LPS induces apoptosis in macrophages mostly through the autocrine production of TNF-alpha, Blood 95 (2000) 3823–3831.

[16] Z. Xing, J. Gauldie, G. Cox, H. Baumann, M. Jordana, X.F. Lei, M.K. Achong, IL-6 is an antiinflammatory cytokine required for controlling local or systemic acute inflammatory responses, J. Clin. Invest. 101 (1998) 311–320.

[17] H. Tilg, E. Trehu, M.B. Atkins, C.A. Dinarello, J.W. Mier, Interleukin-6 (IL-6) as an anti-inflammatory cytokine: induction of circulating IL-1 receptor antagonist and soluble tumor necrosis factor receptor p55, Blood 83 (1994) 113–118.

[18] P. Tremblay, M. Houde, N. Arbour, D. Rochefort, S. Masure, R. Mandeville, G. Opdenakker, D. Oth, Differential effects of PKC inhibitors on gelatinase B and interleukin 6 production in the mouse macrophage, Cytokine 7 (1995) 130–136.

[19] J. Wei, Z. Sun, Q. Chen, J. Gu, Serum deprivation induced apoptosis in macrophage is mediated by autocrine secretion of type I IFNs, Apoptosis 11 (2006) 545–554.

[20] M. Ojaniemi, V. Glumoff, K. Harju, M. Liljeroos, K. Vuori, M. Hallman, Phosphatidylinositol 3-kinase is involved in Toll-like receptor 4-mediated cytokine expression in mouse macrophages, Eur. J. Immunol. 33 (2003) 597–605.

[21] M.J. Díaz-Guerra, A. Castrillo, P. Martín-Sanz, L. Boscá, Negative regulation by phosphatidylinositol 3-kinase of inducible nitric oxide synthase expression in macrophages, J. Immunol. 162 (1999) 6184–6190.

[22] M. Guha, N. Mackman, The phosphatidylinositol 3-kinase-Akt pathway limits lipopolysaccharide activation of signaling pathways and expression of inflammatory mediators in human monocytic cells, J. Biol. Chem. 277 (2002) 32124–32132.

[23] B. Salh, R. Wagey, A. Marotta, J.S. Tao, S. Pelech, A ctivation of phosphatidylinositol 3-kinase, protein kinase B, and p70 S6 kinases in lipopolysaccharide-stimulated Raw 264.7 cells: differential effects of rapamycin, Ly294002, and wortmannin on nitric oxide production, J. Immunol. 161 (1998) 6947–6954.

Nucleic Acids Symposium Series No. 51 409–410
doi:10.1093/nass/nrm205

Expression of shRNA using intron splicing

Kousei Noguchi[2], Yoshio Ishitu[1], Naoko Miyano-Kurosaki[1, 2], and Hiroshi Takaku[1, 2]

[1]Department of Life and Environmental Science and [2]High Technology Research Center, Chiba Institute of Technology, 2-17-1 Tsudanuma, Narashino, Chiba 275-0016, Japan

ABSTRACT

RNA is considered a highly promising candidate for several applications such as gene knock-down, gene repair and gene therapy, where double-stranded RNA and RNA with catalytic activity are key players. A group I intron, a ribozyme catalyzing its own splicing reactions in the absence of any proteins, has generated interest for its potential utility in gene repair using trans-splicing. On the other hand, the induction of small interfering RNA, via double-stranded RNA cleavage in short hairpin RNA (shRNA) by the RNase • •enzyme DICER is a convenient and powerful mechanism for gene silencing. We constructed shRNA expression vectors directed against Firefly luciferase, in which•• the loop region of the shRNA was interrupted by an intron. The decreased levels of luciferase activity were measured in cultured cells as an index of the ribozyme splicing activity.

INTRODUCTION

The group I intron from *Tetrahymena thermophila* catalyzes its own excision and ligation of the 5' and 3' exons; that is, self-splicing without the aid of proteins.[1] Furthermore, self-splicing from an unusual sequence alignment occurs *in vitro* and *in vivo* in other species such as mammals, although group I introns have not been reported in mammals.[2] In addition to self-splicing to ligate two exons juxtaposed to a group I intron, several variants have been developed in which trans-splicing was used to correct gene sequences with mutations, a promising technique for therapeutic use. Several substances interfere with ribozyme activity *in vitro*, including antibiotics. Although low production of final proteins in self-splicing limits its utility, we used the self-splicing mechanism to produce RNA as the final product.

RNA interference (RNAi), which is contingent on cellular factors such as RNA-induced silencing complexes (RISC), is used exclusively for knocking down gene function.[3] The induction of synthetic small interfering RNA (siRNA) or vectors expressing short hairpin RNA (shRNA) into cells is relatively efficient and less demanding.[4] Thus, RNAi is the application of choice to perform high-throughput genetic screening for loss-of function phenotypes in the post-genomic era.[5] Further application of these RNAs for gene regulation is an intriguing possibility to improve conditional gene expression and knock-down systems. Development of these applications, however, is still in progress. In this context, we constructed an expression vector containing an shRNA interrupted by an intron, so that the expressed RNA would be followed by self-splicing of the intron, and the resulting joined transcript was predicted to fold back on itself to form a stem-loop structure, which should produce shRNA (Figure 1).

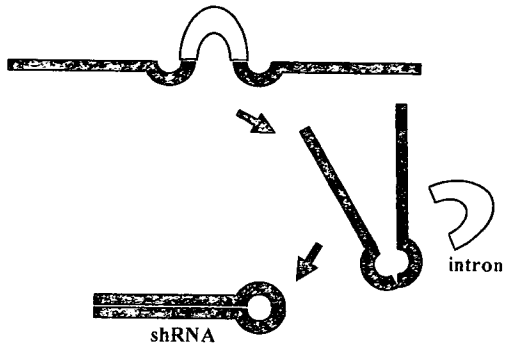

Figure 1. Formation of stem-loop structure through self-splicing of group I intron inserted into the loop site.

RESULTS AND DISCUSSION

To understand the rationale of the construct, shRNA targeting the sequence (155-173) of the firefly luciferase transcript was placed under the CMV promoter, and then a group I intron was inserted into the loop region. Accordingly, the ribozyme activity and shRNA formation were quantitatively analyzed. Because the RNA was longer than the shRNA, it was expected to be fully expressed. Particularly, pol II-driven promoters have a variety of expression patterns, and therefore are more suitable for achieving spatio-temporal expression patterns compared to pol III-driven promoters. Regarding the *Tetrahymena* intron, the sequences of the last moiety of the 5' and 3' exons have a constrained aspect in order to pair with the intron for efficient and precise splicing, namely the P1 helix (5' exon-intron pairing) and P10 helix (intron-3' exon pairing). To accommodate these characteristics, a loop portion that was similar to the pairing sequences was searched for using a microRNA (miRNA) database, and has-mir-371 was selected.[6] In this case, intron sequences were modified in conjunction with the loop (Figure 2).

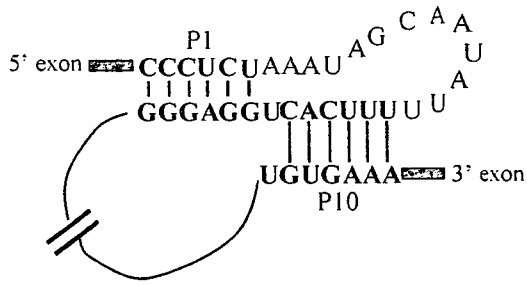

Figure 2. Schematic representation of the interactions involved in self-splicing, with the pairing between the intron and the 5' and 3' exonic sequences.

First, we constructed vectors in which shRNA using the miRNA-derived loop was inserted under the CMV promoter. The efficiency was analyzed by transiently transfecting Hela cells with two vectors expressing *Renilla* luciferase and Firefly luciferase, and luciferase activity was analyzed 60 h after transfection. Reduced Firefly luciferase activity relative to the control vector indicated the usefulness of the vector (Figure 3A; lanes 1, 2). Next, the group I intron was inserted into the middle site of the loop. As expected, when this vector was transiently transfected into Hela cells, decreased Firefly luciferase activity was observed compared to control vectors (Figure 3A; lanes 1, 3). Given that shRNA expression vectors had more profound effects than plasmids expressing shRNA interrupted by an intron, there is room for improvement, such as insertions in the middle of the L1 loop.[7] Moreover, transiently transfected cells were selected under G418 selection, and thereafter we obtained stable cell lines with the plasmid, including the shRNA interrupted by an intron. In accordance with the results obtained from transiently transfected cells, several cell lines showed suppressive effects compared to Hela cells in which two reporter vectors expressing Firefly luciferase and *Renilla* luciferase were cotransfected (Figure 3B; lanes 1, 2, 3). These results imply that continuous expression of the ribozyme is harmless to the cells. The same result was obtained for shRNA targeting the site (850-875) of the luciferase transcript in which the loop domain was similarly interrupted by the intron.

Contrary to several reports that ribozymes are preferentially regulated by several substances *in vitro*, many remain to be validated *in vivo* and others are not working as well as initially expected.[8] Accordingly, our system might control gene expression if it occurs and it might also be useful for screening for ribozymes that are functional *in vivo*. If aptamers are conjoined to the group I intron, the ligand-induced conformational changes might occur *in vivo*.[9]

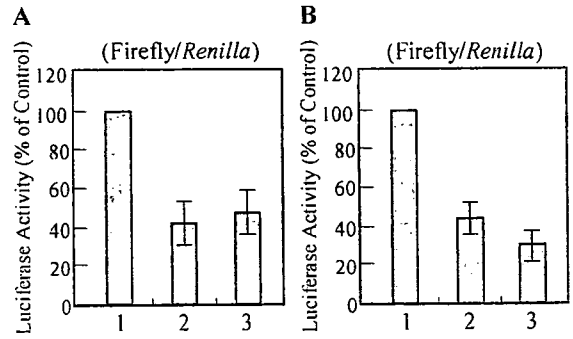

Figure 3. Validation of shRNA and shRNA interruption by the intron using a dual luciferase assay.
A) Lane 1, Empty vector; Lane 2, shRNA expression vectors; Lane 3, Vector with shRNA interrupted by intron B) Lane 1, Hela cells; Lane 2, Clone No.1 within stable cell lines; Lane 3, Clone No.2 within stable cell lines.

CONCLUSION

These results suggested that the CMV promoter can be efficiently used for shRNA expression, and that the miRNA-derived loop is a promising candidate for siRNA production. Furthermore, expression of the integrated RNA comprised of the ribozyme and shRNA is feasible without remarkable toxicity in cultured mammalian cells.

ACKNOWLEDGEMENTS

This work was supported by a Grant-in-Aid for High Technology Research from the Ministry of Education, Science, Sports, and Culture, Japan.

REFERENCES

1. Cech, T.R. (1990) Annu Rev Biochem, 59, 543-568.••
2. Hagen, M., Cech, T.R. (1999) *EMBO J*, 18, 6491-6500.
3. Elbashir, S.M., Harborth, J., Lendeckel, W., Yalcin, A., Weber, K., Tuschl, T. (2001) *Nature*, 411, 494-498.
4. Brummelkamp, T.R., Bernards, R., Agami, R. (2002) *Science*, 296, 550-553.
5. Aza-Blanc, P., Cooper, C.L., Wagner, K., Batalov, S., Deveraux, Q.L., Cooke, M.P. (2003) *Mol Cell*, 12, 627-637.
6. Griffiths-Jones, S., Grocock, R.J., van Dongen, S., Bateman, A., Enright, A.J. (2006) *Nucleic Acids Res*, 34, D140-D144.
7. Hasegawa, S., Jackson, W.C., Tsien, R.Y., Rao, J. (2003) *Proc. Natl Acad. Sci. USA*, 100, 14892-14896.
8. Yen, L., Magnier, M., Weissleder, R., Stockwell, B.R., Mulligan, R.C. (2006) *RNA*, 12, 797-806.
9. Thompson, K.M., Syrett, H.A., Knudsen, S.M., Ellington, A.D. (2002) *BMC Biotechnol*, 2, 1472-6750.

Corresponding Author. E-mail: hiroshi.takaku@it-chiba.ac.jp